GsdmD p30 elicited by caspase-11 during pyroptosis forms pores in membranes

Robin A. Aglietti[a], Alberto Estevez[b], Aaron Gupta[c], Monica Gonzalez Ramirez[d], Peter S. Liu[e], Nobuhiko Kayagaki[c], Claudio Ciferri[b], Vishva M. Dixit[c,1], and Erin C. Dueber[a,1]

[a]Department of Early Discovery Biochemistry, Genentech, Inc., South San Francisco, CA 94080; [b]Department of Structural Biology, Genentech, Inc., South San Francisco, CA 94080; [c]Department of Physiological Chemistry, Genentech, Inc., South San Francisco, CA 94080; [d]Sanford-Burnham Medical Research Institute, La Jolla, CA 92037; and [e]Department of Protein Chemistry, Genentech, Inc., South San Francisco, CA 94080

Contributed by Vishva M. Dixit, May 27, 2016 (sent for review May 17, 2016; reviewed by Thirumala-Devi Kanneganti, Mohamed Lamkanfi, and Ruslan Medzhitov)

Gasdermin-D (GsdmD) is a critical mediator of innate immune defense because its cleavage by the inflammatory caspases 1, 4, 5, and 11 yields an N-terminal p30 fragment that induces pyroptosis, a death program important for the elimination of intracellular bacteria. Precisely how GsdmD p30 triggers pyroptosis has not been established. Here we show that human GsdmD p30 forms functional pores within membranes. When liberated from the corresponding C-terminal GsdmD p20 fragment in the presence of liposomes, GsdmD p30 localized to the lipid bilayer, whereas p20 remained in the aqueous environment. Within liposomes, p30 existed as higher-order oligomers and formed ring-like structures that were visualized by negative stain electron microscopy. These structures appeared within minutes of GsdmD cleavage and released Ca^{2+} from preloaded liposomes. Consistent with GsdmD p30 favoring association with membranes, p30 was only detected in the membrane-containing fraction of immortalized macrophages after caspase-11 activation by lipopolysaccharide. We found that the mouse I105N/human I104N mutation, which has been shown to prevent macrophage pyroptosis, attenuated both cell killing by p30 in a 293T transient overexpression system and membrane permeabilization in vitro, suggesting that the mutants are actually hypomorphs, but must be above certain concentration to exhibit activity. Collectively, our data suggest that GsdmD p30 kills cells by forming pores that compromise the integrity of the cell membrane.

GsdmD | pyroptosis | caspase-11

Pyroptosis is an inflammatory form of programmed cell death that occurs in response to microbial products in the cytoplasm or to cellular perturbations caused by diverse stimuli, including crystalline substances, toxins, and extracellular ATP (1, 2). Pyroptosis plays a critical role in the clearance of intracellular bacteria (3), but may also contribute to autoinflammatory and autoimmune disease pathology. Mechanistically, pyroptosis occurs when cytosolic nucleotide-binding oligomerization domain (NOD)-like receptors (NLRs), including NLRP1, NLRP3, and NLRC4, or the pyrin domain-containing protein AIM2, nucleate a canonical inflammasome complex that activates the protease caspase-1 (2). Alternatively, intracellular lipopolysaccharide (LPS) from Gram-negative bacteria can trigger noncanonical activation of mouse caspase-11 and human caspases 4 and 5 (4–7). Caspases 1, 4, 5, and 11 can each cleave Gasdermin-D (GsdmD) to mediate pyroptotic cell death (8, 9). It is the N-terminal p30 fragment of GsdmD that is cytotoxic to cells, but precisely how it kills cells is unknown.

Here we show that the human GsdmD p30 fragment liberated by active caspase-11 forms ring-like structures within membranes that function as pores. Therefore, we propose p30 kills cells by directly compromising the integrity of cellular membranes. We also show that the GsdmD I105N mutant that was unable to mediate macrophage pyroptosis (9) is hypomorphic at cell killing in a transient overexpression system and at liposome permeabilization in vitro—conditions where p30 concentration favors oligomerization.

Results

Previous studies demonstrated that both endogenous and recombinantly expressed mouse GsdmD were cleaved by caspase-11 (8, 9). We were also able to cleave recombinant human GsdmD with a constitutively active form of caspase-11 lacking the N-terminal caspase activation and recruitment domain (ΔCARDcasp-11; Fig. 1*A*). The resulting N-terminal p30 domain precipitated after cleavage, whereas the C-terminal p20 domain was predominantly soluble (Fig. 1*B*). Given that plasma membrane rupture is a prominent feature of pyroptosis, we hypothesized that the liberated p30 domain favored association with cellular membranes and therefore formed insoluble aggregates in their absence. To test this idea, GsdmD was cleaved by ΔCARDcasp-11 in the presence of liposomes. The resulting reaction was centrifuged over a high-density cushion to float the low-density liposomes and separate them from both the soluble cleavage products and insoluble precipitate (Fig. 1*C*). GsdmD p30, but not GsdmD p20 or full-length GsdmD, strongly colocalized with liposomes of different lipid compositions (Fig. 1 *D* and *E* and Table S1), suggesting that p30 may associate with cellular membranes upon cleavage by caspase-11. Indeed, liposomes composed of either plasma membrane-like or mitochondrial-like lipid bilayers were bound equally well by p30. Interestingly, exclusion of sphingomyelin from the plasma membrane-like liposomes seemed to impair full association of p30 with the membrane (Fig. S1).

Significance

Pyroptosis is a form of cell death that is critical for eliminating innate immune cells infected with intracellular bacteria. Microbial products such as lipopolysaccharide, which is a component of Gram-negative bacteria, trigger activation of the inflammatory caspases 1, 4, 5, and 11. These proteases cleave the cytoplasmic protein Gasdermin-D into two pieces, p20 and p30. The p30 fragment is cytotoxic when liberated from the p20 fragment. Our work suggests that p30 induces pyroptosis by associating with cell membranes and forming pores that perturb vital electrochemical gradients. The resulting imbalance causes the cell to lyse and release intracellular components that can alert other immune cells to the threat of infection.

Author contributions: R.A.A., N.K., V.M.D., and E.C.D. designed research; R.A.A., A.E., A.G., P.S.L., C.C., and E.C.D. performed research; M.G.R. contributed new reagents/analytic tools; R.A.A., A.E., A.G., P.S.L., N.K., C.C., and E.C.D. analyzed data; and R.A.A. and E.C.D. wrote the paper.

Reviewers: T.-D.K., St Jude Children's Research Hospital; M.L., VIB and Ghent University; and R.M., Yale University School of Medicine.

Conflict of interest statement: R.A.A., A.E., A.G., P.S.L., N.K., C.C., V.M.D., and E.C.D. were employees of Genentech, Inc.

Freely available online through the PNAS open access option.

[1]To whom correspondence may be addressed. Email: dixit.vishva@gene.com or dueber.erin@gene.com.

This article contains supporting information online at www.pnas.org/lookup/suppl/doi:10.1073/pnas.1607769113/-/DCSupplemental.

www.pnas.org/cgi/doi/10.1073/pnas.1607769113

Downloaded at Palestinian Territory, occupied on December 14, 2021

www.manaraa.com

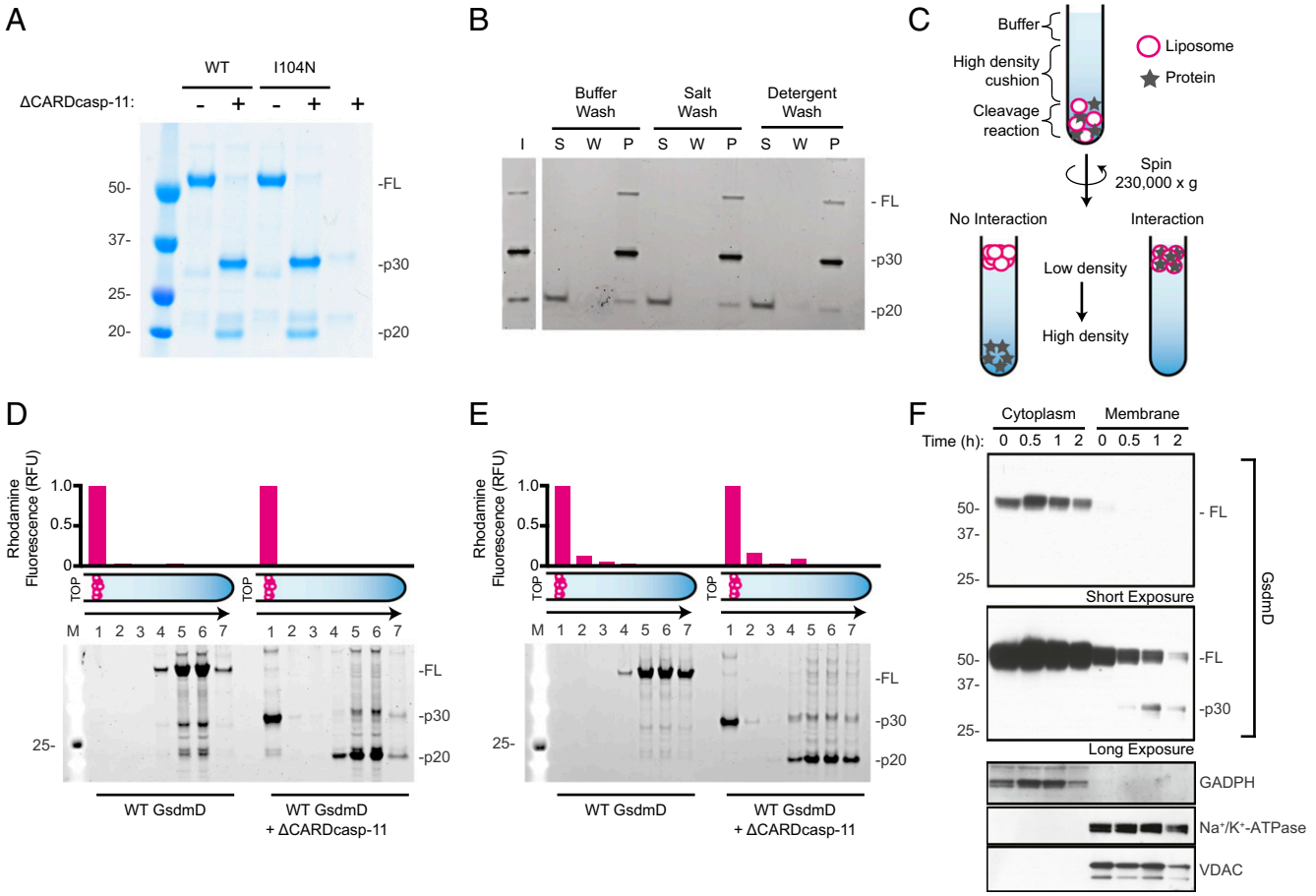

Fig. 1. Processing and membrane partitioning of GsdmD. (*A*) SDS/PAGE of wild-type (WT) and I104N GsdmD with and without ΔCARDcasp-11 treatment (coomassie staining). Full-length (FL) and cleavage products, p20 and p30, are denoted. (*B*) WT GsdmD cleavage reactions were subject to sedimentation analysis to assess component solubilities. SDS/PAGE of input (I), supernatant (S), wash (W), and pellet (P) fractions are shown for different washing strategies (see *SI Methods*, SYPRO ruby staining). (*C*) Schematic of liposome flotation assay. A high-density medium was used to float the low-density liposomes and any associated proteins. Rhodamine-labeled liposomes are shown as magenta circles, and protein is shown as gray stars. (*D* and *E*) Liposome flotation assay fractions were evaluated by SDS/PAGE (SYPRO ruby staining) for reactions containing (*D*) plasma membrane-like and (*E*) mitochondrial-like liposomes. Lanes correspond to successive 100-μL layers starting at the top of the assay tube (*Left* to *Right*) and solubilized pellet (fraction 7). Liposome quantification of each layer (as measured by rhodamine fluorescence, normalized to the top layer) is depicted in the bar graphs above the gels. (*F*) Western blots of immortalized macrophages after stimulation with intracellular LPS. Cellular localization markers, GAPDH (glyceraldehyde 3-phosphate dehydrogenase), Na^+/K^+-ATPase (sodium-potassium adenosine triphosphatase), and VDAC (voltage-dependent ion channel), are shown below.

Next we determined if endogenous GsdmD p30 localized to membranes in immortalized macrophages after caspase-11 activation by electroporated LPS. Cytosolic and membrane-containing fractions were prepared, with p30 only evident in the latter (Fig. 1*F*). In contrast, the majority of full-length GsdmD was detected in the cytosolic fraction, and intracellular LPS did not cause it to accumulate in the membrane fraction. The specificity of our GsdmD antibody was confirmed using GsdmD-deficient bone marrow-derived macrophages (Fig. S2). These data support the notion that GsdmD cleavage by caspase-11 promotes translocation of the GsdmD p30 fragment to cell membranes.

Mutation of isoleucine 105 to asparagine in murine GsdmD was shown to block the cytotoxic activity of GsdmD in mouse macrophages, albeit through an unknown mechanism (9). GsdmD I105N was cleaved by caspase-11 (9); therefore we tested how this mutation affected the membrane association observed for wild-type GsdmD. We confirmed that the corresponding mutation in human GsdmD, I104N, did not impair GsdmD processing by ΔCARDcasp-11 in vitro (Fig. 1*A*). Indeed, wild-type GsdmD and GsdmD I104N were cleaved with very similar kinetics (Fig. 2 *A* and *B*). I104N p30 was also found in the liposome fraction of liposome flotation assays at levels similar to that of wild-type GsdmD, indicating that the mutant is at least competent for membrane association (Fig. 3 *A* and *B*).

We visualized GsdmD p30 on liposomes directly using electron microscopy. GsdmD cleavage reactions were initiated in the presence of liposomes by addition of ΔCARDcasp-11, and then aliquots were applied onto grids at different time-points and subjected to negative staining. Ring-like structures with darkly stained centers were observed embedded in the liposomes (Fig. 4*A*). These structures required processing of GsdmD because they were not observed in liposomes exposed to full-length GsdmD or ΔCARDcasp-11 individually. The ring-like structures appeared within 5 min of initiating the cleavage reaction (Fig. 4*B*). Cleaved GsdmD I104N formed similar structures and on a comparable timescale (Fig. 4*B* and Table 1).

The apparent oligomeric rings were extracted from liposomes using detergent treatment and appeared as a single discrete band at ~720 kDa on a Blue Native-PAGE gel (Fig. 5 and Fig. S3). Mass spectrometry confirmed that the band contained GsdmD p30 (Fig. S3). Based on its molecular weight, this complex should contain about 24 monomers of p30, which is in keeping with the approximate size and stoichiometry of known pore-forming toxins (10–12). Given that pyroptosis is characterized

Downloaded at Palestinian Territory, occupied on December 14, 2021
www.manaraa.com

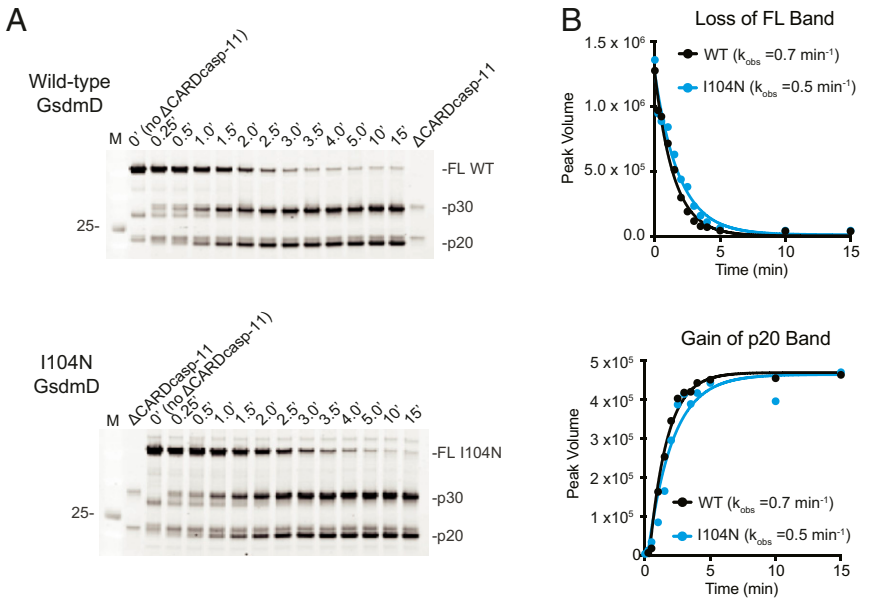

Fig. 2. Kinetics of GsdmD cleavage by ΔCARDcasp-11. (*A*) SDS/PAGE analysis of wild-type (WT) and I104N GsdmD cleavage reaction timecourses (SYPRO ruby staining). (*B*) Quantification of full-length (FL) and p20 bands for WT (black) and I104N (blue) reactions. Single-exponential fits to the data were used to determine listed rates.

by formation of pores in the plasma membrane (13, 14), that ectopic GsdmD p30 kills cells (8, 9), and that the C-terminal domain of another gasdermin family member inhibits toxicity of the corresponding N-terminal domain (15), our observations argue that GsdmD p30 that is liberated by caspase-11 forms pores in cellular membranes.

We performed liposome cargo release assays to more directly assess the effect of p30 association on membrane integrity. Liposomes were loaded with calcium chloride, washed via a desalting column, and then added to a ΔCARDcasp-11–mediated GsdmD cleavage reaction. Subsequent release of calcium ions into the surrounding buffer due to membrane permeabilization was monitored using the calcium-sensitive dye Fura-2. Importantly, loading and subsequent desalting of the liposomes had no effect on p30 membrane localization (Fig. S4). Cleavage of full-length GsdmD into p30 and p20 fragments triggered rapid and robust calcium release from liposomes (Fig. 6 *A* and *B*). The effect was specific to p30 because no calcium was released by GsdmD p20 with ΔCARDcasp-11, by full-length GsdmD alone, or by ΔCARDcasp-11 alone (Fig. S5). GsdmD p30 effectively permeabilized membranes of different lipid composition, albeit at different rates. The fraction of total signal in the assays also varied with liposome type. GsdmD I104N p30 also caused calcium release from liposomes, but at a significantly slower rate than wild-type GsdmD p30 (Fig. 6 *A* and *B*). Dilution of either wild-type or I104N GsdmD retarded the rate of calcium release. However, I104N-mediated membrane permeabilization was more dramatically affected by concentration changes than wild-type (Fig. 6 *C* and *D*). Dilution of both GsdmD variants to submicromolar concentration abrogated observable calcium release in the assay.

Similar trends were also observed for p30-mediated cytotoxicity in cells. Transient transfection of HEK293T cells with wild-type or I105N mouse p30 caused considerable cell death compared with transfection with vector alone (Fig. 7). However, the toxicity of the I105N mutant was attenuated compared with wild-type p30. Attempts to detect expression of the p30 fragments failed, probably due to how fast they killed the cells.

Discussion

Plasma membrane permeabilization is a hallmark of pyroptotic cell death (13, 14). A study of *Salmonella*-infected macrophages estimated functional pyroptotic pores to be 1.1–2.4 nm in diameter based on the size range of osmoprotectant molecules that prevented cell lysis (13). It was surmised that pores of this size would disrupt ionic gradients and cause water influx, cell swelling, and eventual membrane rupture. Direct imaging of GsdmD p30 pores by negative

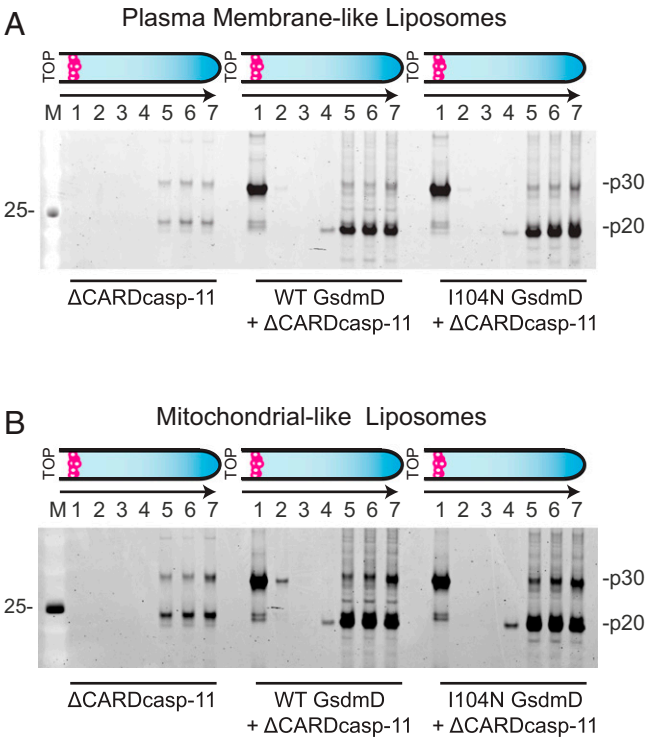

Fig. 3. GsdmD colocalization with different membrane compositions. Rhodamine-labeled (*A*) plasma membrane-like and (*B*) mitochondrial-like liposomes were incubated with wild-type (WT) and I104N cleavage reactions or with ΔCARDcasp-11 alone. Liposomes were separated via flotation assay, and the resulting layers were analyzed by SDS/PAGE (SYPRO ruby staining). GsdmD p20 and p30 cleavage products are denoted.

Downloaded at Palestinian Territory, occupied on December 14, 2021
www.manaraa.com

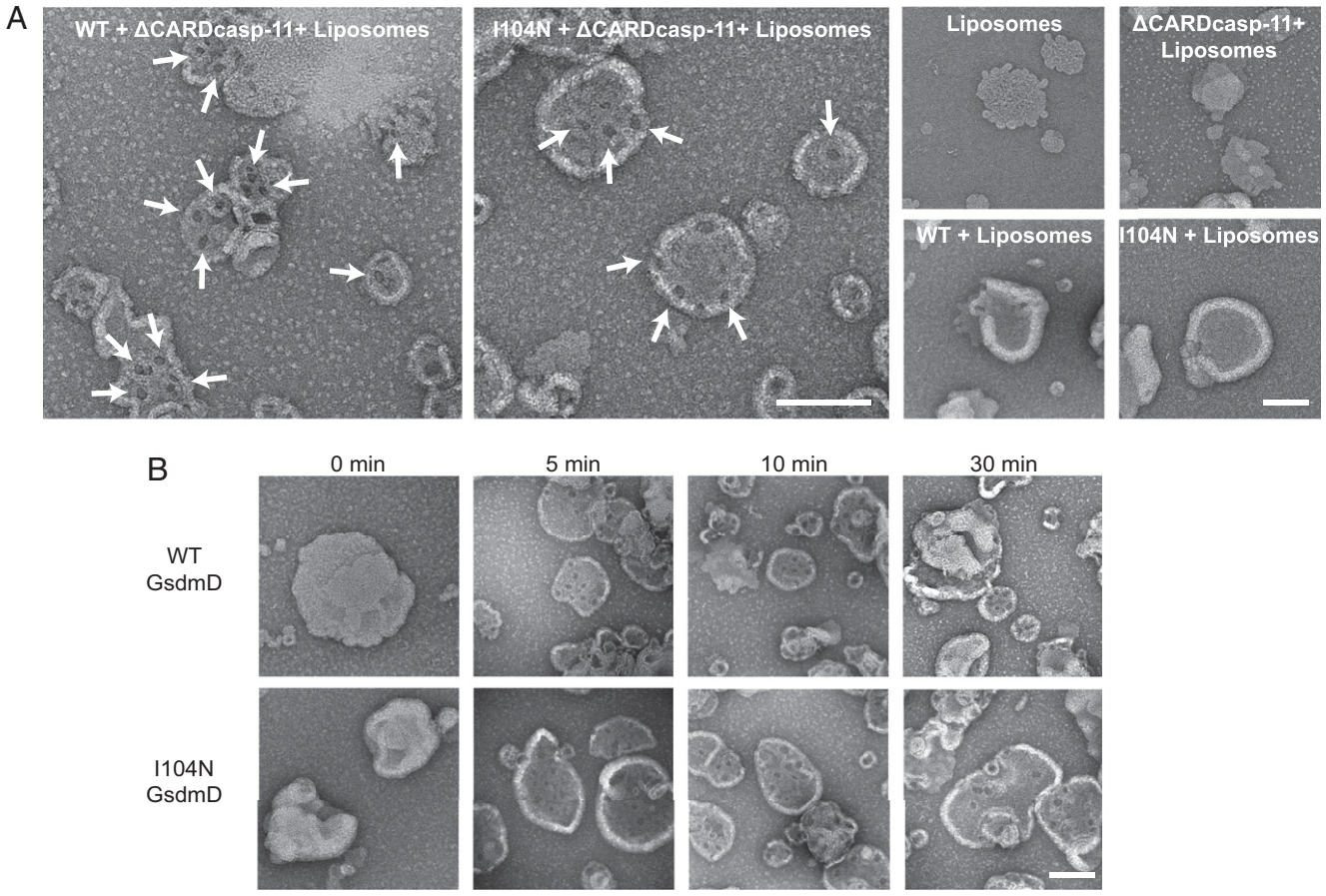

Fig. 4. Negative stain electron microscopy images of p30-bound liposomes. (*A*) Representative images of liposomes incubated with GsdmD cleavage reactions and control samples. Ring-shaped pore structures are highlighted with arrows. (*B*) Images from a timecourse of GsdmD cleavage reactions initiated by ΔCARDcasp-11. (Scale bar for all images, 100 nm.)

stain electron microscopy revealed ring-shaped oligomers with an average inner diameter of ~13 nm (Table 1). Pores of these dimensions might do more than just permeabilize membranes to ions, as shown using liposome cargo release assays (Fig. 6). They would also be theoretically large enough for secretion of the proinflammatory cytokines interleukin (IL)-1β and IL-18. These cytokines are cleaved by caspase-1 into their mature, active forms, but they lack sorting motifs for secretion via the classical ER-Golgi secretory pathway. Therefore, it is tempting to speculate that IL-1β and IL-18 could exit the pyroptotic cell through GsdmD p30 pores even before catastrophic membrane rupture by osmotic lysis.

We observed p30 membrane association and permeabilization with both plasma membrane-like and mitochondrial-like liposomes. Whereas p30 membrane localization appeared equivalent for the two lipid compositions in longer timescale liposome flotation assays, p30-mediated calcium release was more rapid and efficient with the mitochondrial-like lipid bilayers. It has been reported that inflammasome activation leads to caspase-1–dependent mitochondrial damage (16). Our findings suggest that formation of GsdmD p30 pores in mitochondrial membranes may account for the observed organelle damage.

Previous work has shown that specific lipids can modulate insertion and/or nucleation of pore-forming toxins (17–20). Our data demonstrate that p30 can bind and permeabilize liposomes of disparate lipid composition, although the rate of calcium release and fraction of total signal in the liposome release assays varied with liposome type (Fig. 6). These data indicate that there is a rate-limiting

Table 1. Diameter of ring-like structures visualized by electron microscopy

	Inner pore diameter (nm)	StDev (nm)*
Wild-type GsdmD	12.8	2.4
I104N GsdmD	13.6	2.4

*n = 50 for both wild-type and I104N.

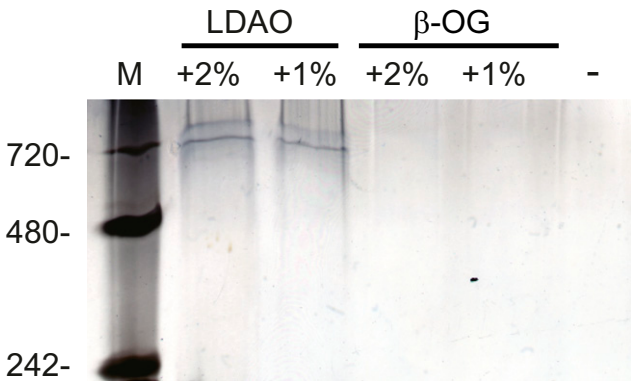

Fig. 5. Blue Native-PAGE analysis of p30 colocalized to membranes. Liposome-bound p30 was treated with detergent and analyzed by BN-PAGE along with a no-detergent control. Bands were visualized by silver staining. LDAO (n-Dodecyl-N,*N*-Dimethylamine-*N*-Oxide) and β-OG (n-Octyl-β-Glucoside).

Downloaded at Palestinian Territory, occupied on December 14, 2021
www.manaraa.com

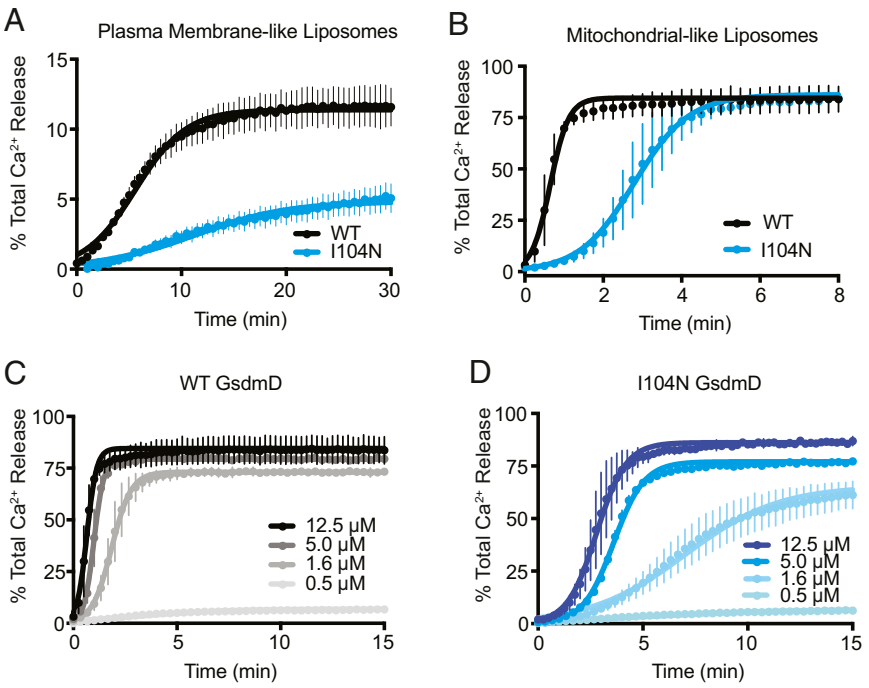

Fig. 6. Calcium-loaded liposome release assays. Calcium release from (*A*) plasma membrane-like and (*B*) mitochondrial-like liposomes upon incubation with ΔCARDcasp-11 and full-length wild-type (WT) or I104N GsdmD (mean ± SD error bars; $n = 6$). Dilution series of (*C*) WT and (*D*) I104N GsdmD in calcium release assays from loaded mitochondrial-like liposomes (mean ± error bars; $n = 3$). All fits shown are standard logistic function.

step between p30 membrane binding and functional pore formation that is affected by lipid composition, presumably either p30 oligomerization or penetration into the lipid bilayer itself. Sphingomyelin is a lipid that gathers into lipid rafts (21, 22), and its exclusion from liposomes appeared to hinder effective p30 association with membranes in coflotation assays. However, sphingomyelin was not required for p30 colocalization with liposomes that contained cardiolipin, another lipid that forms raft-like microdomains (23, 24). Taken together, our data suggest that lipid composition probably influences p30 insertion into the membrane, with lipids that create boundaries or physical distortions in the lipid bilayer facilitating membrane entry.

Irrespective of liposome composition, the I104N mutant p30 colocalized with membranes similar to wild-type p30, but demonstrated slower calcium release from loaded liposomes (Fig. 6). Given that full-length wild-type and I104N GsdmD were cleaved by ΔCARDcasp-11 at similar rates in vitro (Fig. 2), I104N dysfunction appears to be intrinsic to the mutant GsdmD itself rather than affecting interactions with another protein in the signaling cascade. Collectively, our data suggest that the I104N mutation directly impedes p30 pore formation. It is possible that the I104N mutant is defective at membrane insertion, but the permeabilization kinetics would also be consistent with impaired p30 oligomerization.

Our data are consistent with an oligomerization model in which formation of a small, stable "seed" is a rate-limiting step before full assembly into the final ring-like oligomer (25). If the I104N point mutation weakens p30 self-association, this would impair p30 oligomerization by effectively raising the threshold concentration required to form a stable seed. Such a defect could be overcome by increasing the concentration of the mutant. This model may explain why the endogenous I105N mouse mutant blocked noncanonical pyroptosis in macrophages, similar to GsdmD deficient cells (9), but had hypomorphic cell lytic activity when overexpressed in HEK293T cells (Fig. 7). Moreover, nonassembled or improperly assembled mutant p30 fragments would likely contain exposed hydrophobic surfaces and, thus, may be more susceptible to the cell's quality control mechanisms.

Although the molecular details of p30 assembly and membrane insertion remain to be fully elucidated, our studies indicate a direct role for GsdmD p30 in the formation of pyroptotic pores. Caspase-11 cleavage of GsdmD very effectively removes the inhibitory C-terminal p20 fragment, allowing p30 to assemble into functional pores. The pronounced segregation of p30 and p20 populations, especially in the presence of membranes, suggests that at least one of these newly formed fragments undergoes conformational rearrangements that favor dissociation, as opposed to just a simple covalent decoupling upon proteolytic cleavage. A more detailed understanding of p30-p20 interactions in the autoinhibited full-length protein would enable identification/design of mutations that either impede or enhance GsdmD cytotoxicity. Such mutations would be important tools in probing the molecular

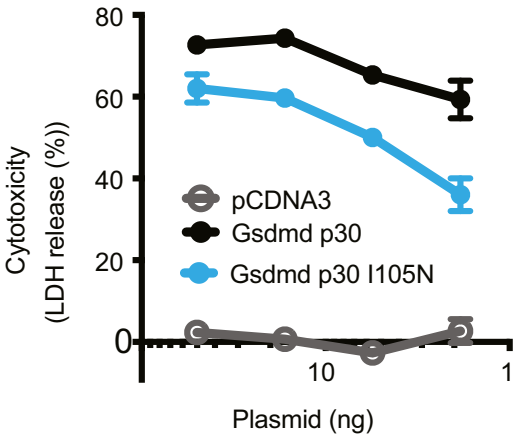

Fig. 7. Cytotoxicity of GsdmD p30 variants. Cytotoxicity, as measured by lactate dehydrogenase (LDH) release, at 24 h after transient transfection of HEK293T cells. Graph shows the mean ± SD of triplicate wells and is representative of three independent experiments.

Downloaded at Palestinian Territory, occupied on December 14, 2021
www.manaraa.com

mechanisms of p30 inhibition and oligomerization and may also provide important insights into how the cytotoxic p30 domains from the other gasdermin family members (26) are regulated.

Methods

Full-length GsdmD variants were expressed in insect cells and purified to homogeneity. Recombinant ΔCARDcasp-11 was added to process GsdmD into its p30 and p20 fragments. Synthetic liposomes were used to evaluate p30 membrane association and pore formation. Localization of endogenous p30 to cellular membranes was determined by cellular fractionation of LPS-stimulated bone marrow-derived macrophages. Detailed methods are provided in *SI Methods*.

ACKNOWLEDGMENTS. We thank Irma Stowe, Bettina Lee, and Mike Holliday for technical assistance; Joyce Lai for assistance with anti-GsdmD antibody reagents; Kim Newton for editing of the manuscript; and Guy Salvesen for helpful discussions. We also thank the BioMolecular Expression Group for construct generation, expression analysis, and large-scale expression.

1. Cookson BT, Brennan MA (2001) Pro-inflammatory programmed cell death. *Trends Microbiol* 9(3):113–114.
2. Lamkanfi M, Dixit VM (2014) Mechanisms and functions of inflammasomes. *Cell* 157(5):1013–1022.
3. Miao EA, et al. (2010) Caspase-1-induced pyroptosis is an innate immune effector mechanism against intracellular bacteria. *Nat Immunol* 11(12):1136–1142.
4. Kayagaki N, et al. (2011) Non-canonical inflammasome activation targets caspase-11. *Nature* 479(7371):117–121.
5. Kayagaki N, et al. (2013) Noncanonical inflammasome activation by intracellular LPS independent of TLR4. *Science* 341(6151):1246–1249.
6. Hagar JA, Powell DA, Aachoui Y, Ernst RK, Miao EA (2013) Cytoplasmic LPS activates caspase-11: Implications in TLR4-independent endotoxic shock. *Science* 341(6151): 1250–1253.
7. Shi J, et al. (2014) Inflammatory caspases are innate immune receptors for intracellular LPS. *Nature* 514(7521):187–192.
8. Shi J, et al. (2015) Cleavage of GSDMD by inflammatory caspases determines pyroptotic cell death. *Nature* 526(7575):660–665.
9. Kayagaki N, et al. (2015) Caspase-11 cleaves gasdermin D for non-canonical inflammasome signalling. *Nature* 526(7575):666–671.
10. Dal Peraro M, van der Goot FG (2016) Pore-forming toxins: Ancient, but never really out of fashion. *Nat Rev Microbiol* 14(2):77–92.
11. Tilley SJ, Orlova EV, Gilbert RJ, Andrew PW, Saibil HR (2005) Structural basis of pore formation by the bacterial toxin pneumolysin. *Cell* 121(2):247–256.
12. Leung C, et al. (2014) Stepwise visualization of membrane pore formation by suilysin, a bacterial cholesterol-dependent cytolysin. *eLife* 3:e04247.
13. Fink SL, Cookson BT (2006) Caspase-1-dependent pore formation during pyroptosis leads to osmotic lysis of infected host macrophages. *Cell Microbiol* 8(11):1812–1825.
14. Bergsbaken T, Fink SL, Cookson BT (2009) Pyroptosis: Host cell death and inflammation. *Nat Rev Microbiol* 7(2):99–109.
15. Lin HY, Lin PH, Wu SH, Yang LT (2015) Inducible expression of gasdermin A3 in the epidermis causes epidermal hyperplasia and skin inflammation. *Exp Dermatol* 24(11): 897–899.
16. Yu J, et al. (2014) Inflammasome activation leads to Caspase-1-dependent mitochondrial damage and block of mitophagy. *Proc Natl Acad Sci USA* 111(43): 15514–15519.
17. Giddings KS, Johnson AE, Tweten RK (2003) Redefining cholesterol's role in the mechanism of the cholesterol-dependent cytolysins. *Proc Natl Acad Sci USA* 100(20): 11315–11320.
18. Shimada Y, Maruya M, Iwashita S, Ohno-Iwashita Y (2002) The C-terminal domain of perfringolysin O is an essential cholesterol-binding unit targeting to cholesterol-rich microdomains. *Eur J Biochem* 269(24):6195–6203.
19. Waheed AA, et al. (2001) Selective binding of perfringolysin O derivative to cholesterol-rich membrane microdomains (rafts). *Proc Natl Acad Sci USA* 98(9):4926–4931.
20. Abrami L, van Der Goot FG (1999) Plasma membrane microdomains act as concentration platforms to facilitate intoxication by aerolysin. *J Cell Biol* 147(1): 175–184.
21. Brown DA, Rose JK (1992) Sorting of GPI-anchored proteins to glycolipid-enriched membrane subdomains during transport to the apical cell surface. *Cell* 68(3):533–544.
22. Zech T, et al. (2009) Accumulation of raft lipids in T-cell plasma membrane domains engaged in TCR signalling. *EMBO J* 28(5):466–476.
23. Renner LD, Weibel DB (2011) Cardiolipin microdomains localize to negatively curved regions of Escherichia coli membranes. *Proc Natl Acad Sci USA* 108(15):6264–6269.
24. Sorice M, et al. (2009) Cardiolipin-enriched raft-like microdomains are essential activating platforms for apoptotic signals on mitochondria. *FEBS Lett* 583(15):2447–2450.
25. Oosawa F, Asakura S (1975) *Thermodynamics of the Polymerization of Protein* (Academic Press, New York).
26. Tamura M, et al. (2007) Members of a novel gene family, Gsdm, are expressed exclusively in the epithelium of the skin and gastrointestinal tract in a highly tissue-specific manner. *Genomics* 89(5):618–629.
27. Hildebrand JM, et al. (2014) Activation of the pseudokinase MLKL unleashes the four-helix bundle domain to induce membrane localization and necroptotic cell death. *Proc Natl Acad Sci USA* 111(42):15072–15077.

Downloaded at Palestinian Territory, occupied on December 14, 2021

www.manaraa.com